



Contents lists available at ScienceDirect

Bioresource Technology

journal homepage: www.elsevier.com/locate/biortech



Accelerated methanogenesis from effluents of hydrogen-producing stage in anaerobic digestion by mixed cultures enriched with acetate and nano-sized magnetite particles



Zhiman Yang^{a,1}, Xiaohui Xu^{a,1}, Rongbo Guo^{a,*}, Xiaolei Fan^a, Xiaoxian Zhao^{a,b}

^a Key Laboratory of Biofuels, Qingdao Institute of Bioenergy and Bioprocess Technology, Chinese Academy of Sciences, Qingdao 266101, China

^b College of Chemical Science and Engineering, Qingdao University, Qingdao 266071, China

HIGHLIGHTS

- The paddy soil enrichments degrading acetate were obtained via magnetite addition.
- Magnetite significantly accelerated methane production from acetate.
- *Rhodocyclaceae*-related species were selectively enriched with magnetite addition.
- Enrichments can rapidly convert the effluents of hydrogen-producing stage to methane.

ARTICLE INFO

Article history:

Received 12 March 2015

Received in revised form 13 April 2015

Accepted 16 April 2015

Available online 22 April 2015

Keywords:

Anaerobic digestion

Magnetite

Acetate

Rhodocyclaceae

ABSTRACT

Potential for paddy soil enrichments obtained in the presence of nano-sized magnetite particles (named as PSEM) to promote methane production from effluents of hydrogen-producing stage in two-stage anaerobic digestion was investigated. The results showed that the addition of magnetite significantly accelerated methane production from acetate in a dose-independent manner. The results from high-throughput sequencing analysis revealed that *Rhodocyclaceae*-related species were selectively enriched, which were likely the key players for conversion of acetate to methane in PSEM. Compared to the paddy soil enrichments obtained in the absence of magnetite (named as PSEC), the maximum methane production rate in PSEM was significantly higher (1.5–5.5 times higher for the artificial medium and 0.2–1.7 times higher for the effluents). The accelerated methane production from the effluents indicated remarkably application potential of PSEM for improving performance of anaerobic digestion.

© 2015 Elsevier Ltd. All rights reserved.

1. Introduction

Anaerobic digestion (AD) is a commonly employed bioenergy technology to produce methane from organic solid wastes. However, low efficiency and long retention times (30–200 days), which usually occur in traditional one-stage AD, prevent its practical applicability (Kwietniewska and Tys, 2014; Ruile et al., 2015). In tackling these questions, researchers have focused on development of a two-stage AD to separate acidogenesis (hydrogen-producing stage) and methanogenesis (methane-producing stage) (Merlino et al., 2013; Yang et al., 2011). This body of works demonstrate the potentially significant role of the two-stage AD in

enhancing biogas yield and improving stability of the process. Despite of these advantages, application of the two-stage AD has been restricted due to long retention times (20–36 days) and low methane production rate (Dareioti and Kornaros, 2014; Massanet-Nicolau et al., 2013). It is known that considerable volatile fatty acids (VFAs) (e.g. propionate and butyrate) produced in the hydrogen-producing stage were converted slowly to the methanogenic substrate (e.g. acetate and H₂) in the methane-producing stage (Wang et al., 2009). Thus, enhancing the degradation rate of VFAs might provide a reduction of long retention times during the two-stage AD.

Effective interspecies electron transfer (IET) is a vital process in AD, constructing basis of syntrophic relationship between fermentative bacteria and methanogen (Sieber et al., 2012). It has been reported that conductive materials (e.g. iron oxides) were capable of enhancing methane production rate via facilitating IET between bacteria and methanogens (Kato et al., 2012; Zhou et al., 2014).

* Corresponding author. Tel./fax: +86 532 80662708.

E-mail address: guorb@qibebt.ac.cn (R. Guo).

¹ These authors contributed equally to this work and should be considered co-first authors.

This led to a central hypothesis that promoting IET might accelerate methane production from VFAs in the methane-producing stage of the two-stage AD.

Nano-sized magnetite particles added to paddy soil resulted in a significant increase in methane production rate (over 30%) from acetate, concomitant with specific enrichment of *Geobacter* and *Methanosarcina* (Kato et al., 2012; Zhou et al., 2014). These findings all demonstrate potentially value of the paddy soil enrichments obtained in the presence of nano-sized magnetite particles (named as PSEM) on accelerating methane production in AD. However, to best of knowledge, no attempts have been made to identify the potential of PSEM for application on the methane-producing stage of the two-stage AD. In this work, the methanogenic characteristics of PSEM were assessed in detail, which led to draw a conclusion that PSEM can serve as improving methane-producing rate for the methane-producing stage of the two-stage AD.

2. Methods

2.1. Paddy soil samples and preparation of nano-sized magnetite particles

Paddy soil samples collected from a rice field (Guangzhou, China) were used as inocula. Total solids (TS) content of the soil samples was 61% (w/w), which contained 8.12% of volatile solids (VS). Nano-sized magnetite particles (8–10 nm) were prepared by slowly adding an acidic solution containing Fe(II) and Fe(III) into NaOH solution under anaerobic conditions (Kang et al., 1996). X-ray diffraction (XRD) analysis showed the resulted products as magnetite.

2.2. Methane production

Batch experiments were carried out at 30 °C in 120 mL anaerobic bottles with 50 mL of working volume, except for experiments 2 and 3, where 20 mL of working volume in 60 mL bottles was used. Each experimental group was performed in triplicate without shaking. Both the inocula and medium were loaded into the bottles, which were then purged with 99.99% of N₂ and closed with butyl rubber stoppers. The initial pH values for all experiments were adjusted to 7.0. The medium (per liter) consisted of 1 g NaH₂PO₄·H₂O, 0.55 g Na₂HPO₄·H₂O, 3 g NaHCO₃, 275 mg CaCl₂, 310 mg NH₄Cl, 330 mg MgCl₂, 130 mg KCl, 5 mg MnCl₂, 10 mg FeCl₃·7H₂O, 0.1 mg CuCl₂·5H₂O, 1 mg CoCl₂·5H₂O, 28 mg NiCl₂, 1 mg ZnCl₂, 0.1 mg H₃BO₃, 0.25 mg Na₂MoO₄, 0.24 mg NiCl₂·6H₂O, and 1 mg EDTA.

Semi-continuous enrichment cultivations (experiment 1) were performed to obtain PSEM. 1.5 g of soil samples were mixed with 50 mL of sterile medium containing 20 mM acetate and 20 mM magnetite. 5 mL of enrichments were transferred into 45 mL of fresh medium amended with 20 mM acetate and 20 mM magnetite when each generation had the highest methane yield. Five generations of subculture were conducted.

In experiments 2 and 3, the resulted enrichments from the fifth generation were used as inocula at the concentration of 0.11 g-VS/L. Experiment 2 was used to detect effects of initial magnetite concentrations (ranging from 20 to 320 mM) on methane production from 20 mM of acetate. The effects of initial acetate concentrations (ranging from 20 to 200 mM) on methanogenesis were evaluated in experiment 3.

Repeated batch cultivation (experiment 4) was conducted to examine the performance of PSEM on degradation of effluent from the hydrogen-producing stage of the two-stage AD. Artificial medium and effluents from hydrogen-producing stage of *Macrocystis pyrifera* biomass residues were used. Total amounts of ethanol and VFAs (270 mM) in the artificial medium consisted of ethanol

(40.7%), acetate (22.6%), propionate (19.3%) and butyrate (16.8%). Total VFAs and ethanol (201 mM) in the effluents obtained through centrifugation at 4000 rpm were composed of acetate (48.1%), propionate (10.2%), butyrate (28.8%), valerate (12.2%), caproate (0.7%) and trace amounts of ethanol. In the start-up incubation stage, 0.11 g-VS/L of the resulted enrichments from the fifth generation were grown in the medium containing 20 mM acetate and 20 mM magnetite. When methane production ceased, 20% (v/v) of the medium was withdrawn and replaced with the same amounts of the effluents or the artificial medium. Biogas remained in headspace of bottles was withdrawn using a vacuum pump and replaced with high purity N₂ before start of the next cycle. For the repeated batch experiments, the mixed cultures from the first cycle that had the highest methane production were used as the inocula for the second cycle of cultivation. Two cycles of harvesting and nutrient feeding were performed.

2.3. Analytical methods

The volume of produced biogas was determined using water displacement method. The fraction of CH₄ in the produced biogas was periodically measured using gas chromatograph (SP6890, Shandong, China) equipped with a thermal conductivity detector according to methods of Yang et al. (2011). Concentrations of ethanol and individual VFAs were determined with high performance liquid chromatography (Agilent HPLC 1200 series) equipped with UV detection (210 nm), refractive index detection and Aminex HPX-87P cation exchange column (Bio-Rad Laboratories, Hercules, CA). 5 mM of H₂SO₄ was used as the mobile phase. The flow rate was 0.6 mL/min with the column temperature of 65 °C. According to the standard methods (APHA, 1998), TS of the samples were measured after drying at 105 °C for 12 h in an oven, then VS of the samples was measured after igniting at 550 °C for 2 h in a muffle furnace. The maximum methane production rate (R_m) and the lag-phase time (λ) in each batch experiment were depicted by the modified Gompertz equation (Yang et al., 2011). The methane yield (P_s) was calculated by dividing cumulative methane production with total acetate used.

2.4. DNA extraction, PCR amplification and 16S rDNA sequencing

Samples from the fifth generation of enrichments were collected for DNA extraction. Total genomic DNA was extracted according to a CTAB/SDS method. PCR was conducted on Thermal Cycler (Bio-rad T100) with bacterial primer pair (515f/806r) for V4 region of 16S rRNA (Peiffer et al., 2013). 30 µL of PCR reaction volume consisted of 15 µL of Phusion® High-Fidelity PCR Master Mix (New England Biolabs), 0.2 µM of forward and reverse primers, and about 10 ng of template DNA. Thermal cycles consisted of initial denaturation at 98 °C for 1 min, followed by 30 cycles of denaturation at 98 °C for 10 s, annealing at 50 °C for 30 s, and elongation at 72 °C for 30 s, followed by a final step at 72 °C for 5 min. PCR products were purified using GeneJET Gel Extraction Kit (Thermo Scientific). Then the purified PCR products were used for sequencing libraries preparation using NEB Next® Ultra™ DNA Library Prep Kit for Illumina (NEB, USA). The library quality was assessed on the Qubit® 2.0 Fluorometer (Thermo Scientific) and Agilent Bioanalyzer 2100 system. Finally, the library was sequenced on an Illumina MiSeq platform.

Raw tags were produced from the merged paired-end reads using FLASH (Magoč and Salzberg, 2011). To obtain clean tags, the low quality sequences and chimeras were filtered, trimmed and removed using the Quantitative Insights into Microbial Ecology (QIIME software v1.3.0) pipeline (Caporaso et al., 2010) and UCHIME Algorithm (Edgar et al., 2011). FASTAQ formatted of clean tags have been submitted to the GeneBank Sequence Read

Archive with accession No. SRR1832302. The clean tags were clustered into operational taxonomic units (OTUs) by setting a 0.03 distance limit using the Uparse program (Edgar, 2013). The taxonomy of OTU representative sequences were phylogenetically assigned to taxonomic classifications by RDP Classifier (Wang et al., 2007) and Greengenes (DeSantis et al., 2006) with a confidence threshold of 80%. Rarefaction curves, Shannon diversity index and species richness estimator of CHAO1 were obtained using MOTHUR program (http://www.mothur.org/wiki/Main_Page).

3. Results and discussion

3.1. Paddy soil enrichments and their characteristics

To test the hypothesis that promoting IET might accelerate methanogenesis in the methane-producing stage of the two-stage AD, PSEM was firstly established. Cumulative methane production during semi-continuous enrichment cultivation is shown in Fig. 1. Time course of methane production in PSEM was always shorter (23% shorter in the first generation, 44% shorter in the second generation, 48% shorter in the third generation, 29% shorter in the fourth generation and 35% shorter in the fifth generation) than in the corresponding paddy soil enrichments obtained in the absence of magnetite (named as PSEC). PSEM produced about 21 mL of methane from acetate that was similar to the results observed in PSEC over each generation of incubation. These findings indicated that magnetite was not capable of enhancing the amount of methane ultimately produced from acetate. The similar phenomena in paddy soil enrichments supplemented with magnetite and acetate have also been reported by Kato et al. (2012), which showed that the addition of magnetite led to no improvement in the ultimate amount of methane.

As shown in Table 1, the methane yield from acetate was average 0.96 mol CH₄/mol acetate. According to the equation (CH₃COO[−] + H₂O → CH₄ + HCO₃[−]), the value presented in this work was close to the theoretical value (1 mol CH₄/mol acetate). This showed that acetate was nearly completely converted to methane.

Table 1 also shows that the addition of magnetite led to the accelerated methane production in terms of the maximum methane production rate and the lag-phase time. In the first generation, the maximum methane production rate of PSEM was 61.2% higher than that of PSEC. Similar results were also observed in the subsequent four generations of subculture. As for each generation of enrichment, the lag-phase time of methane production in PSEM showed a reduction that is always shorter than that in the corresponding PSEC. Additionally, Fig. 2 shows that the addition of magnetite accelerated the metabolism of acetate concomitant with the rapid methane production. These results, combined with the observations that magnetite promoted methane production rate, suggested that the addition of magnetite can promote rates of acetate conversion to methane. In agreement with the observations in present study, recent studies on batch incubation of paddy soil enrichments revealed a significant increase in methane production rate (over 30%) by adding nano-sized magnetite particles (Kato et al., 2012; Zhou et al., 2014).

To further evaluate methanogenic characteristics of the paddy soil enrichments, the effects of different concentrations of magnetite or acetate on methanogenesis were measured. Increasing the magnetite concentration resulted in no significant changes

Table 1

Methane yield, methane production rate and lag-phase time in the semi-continuous enrichment cultivation.

	Ps (mol CH ₄ /mol-acetate)	Rm (mmol/d)	λ (d)	R ²
<i>PSEC</i>				
Generation 1	0.91 ± 0.01	0.067	9.23	0.99
Generation 2	0.93 ± 0.08	0.069	7.07	0.99
Generation 3	0.98 ± 0.03	0.122	7.14	0.98
Generation 4	0.90 ± 0.01	0.054	5.07	0.99
Generation 5	1.00 ± 0.01	0.047	6.76	0.99
<i>PSEM</i>				
Generation 1	0.98 ± 0.01	0.108	8.87	0.99
Generation 2	0.95 ± 0.04	0.181	5.21	0.99
Generation 3	0.97 ± 0.01	0.154	4.34	0.98
Generation 4	0.89 ± 0.02	0.079	4.27	0.99
Generation 5	0.99 ± 0.01	0.074	4.96	0.99

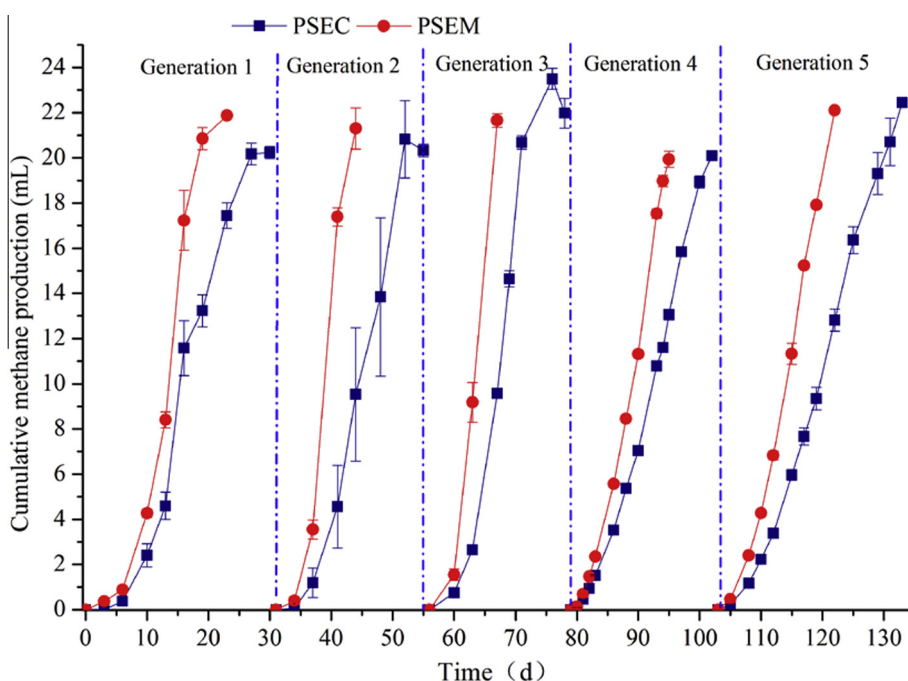


Fig. 1. Profiles of cumulative methane production from acetate in the semi-continuous enrichment cultivation.

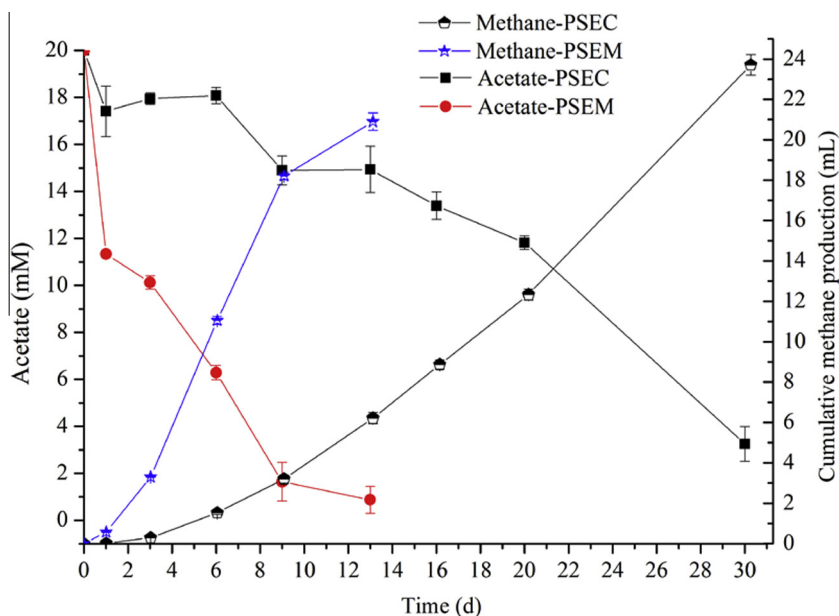


Fig. 2. Time course of acetate conversion to methane.

Table 2

Kinetic parameters for methane production at different magnetite concentrations.

Magnetite (mM)	Rm (mmol/d)	λ (d)	Ps (mol CH ₄ /mol-acetate)	R ²
20	0.129	1.52	0.97 ± 0.02	0.99
80	0.117	1.32	0.96 ± 0.03	0.99
160	0.114	1.32	0.97 ± 0.01	0.99
320	0.103	1.35	1.00 ± 0.03	0.99

in the lag-phase time, the methane yield and production rate (Table 2). These results indicated that the magnetite accelerated methanogenesis from acetate in a dose-independent manner when its concentrations >20 mM. Table 3 shows that the maximum methane production rate slightly increased with the acetate concentrations up to 50 mM, while no significant improvement in methane production rate was observed at the acetate concentrations >50 mM. Increasing acetate concentrations led to a stepwise decrease in the methane yield as well as a stepwise extension in the lag-phase time. These results showed that the high concentration of acetate might lead to inhibition on methane production. Fukuzaki et al. (1990a) reported that the undissociated form of acetic acid can inhibit the growth and metabolism of acetate-utilizing bacteria. In this work, increasing the initial acetate concentration from 20 to 200 mM resulted in the increase in undissociated form of acetic acid from 0.114 to 1.144 mM (Table 3). Thus, the methanogenic inhibition might attribute to the toxicity of the undissociated form of acetic acid to the cells.

Table 3

Concentration of initial undissociated acetic acid and kinetic parameters for methane production at different initial acetate concentrations.

Acetate (mM)	Undissociated acetic acid ^a (mM)	Rm (mmol/d)	λ (d)	Ps (mol CH ₄ /mol-acetate)	R ²
20	0.114	0.14	1.8	0.88 ± 0.05	0.99
50	0.286	0.21	2.3	0.87 ± 0.05	0.99
100	0.572	0.21	3.02	0.70 ± 0.17	0.99
200	1.144	0.16	5.48	0.36 ± 0.01	0.99

^a Calculated by using a pK_a of 4.76 at 30 °C and pH 7.

3.2. Structure of microbial communities

The bacterial diversities of the paddy soil enrichments in the fifth generation were evaluated using the 16S rRNA amplicon sequencing. A small portion of archaeal sequences were recovered, due to non-specificity of primer pair targeting V4 region of bacterial 16S rRNA genes. Species richness of bacterial communities was evaluated using rarefaction analysis. As shown in Fig. 3, the rarefaction curves of two samples approached, but did not achieve, a plateau, indicating that the sequencing depths did not fully cover the diversity of the bacterial communities. However, the coverage values (>97%) showed that most common OTUs were embraced (Table 4). The OTUs, CHAO1 richness and Shannon index of bacterial community in PSEC was higher than that in PSEM, indicating that PSEC had higher diversity in bacterial species. These results indicated that the supplementation of magnetite to the paddy soil reduced the diversity of bacterial communities.

Fig. 4 shows the phylogenetic classification of bacterial OTUs at the family level. A similar percentage of *Dethiosulfovibrionaceae*, in which *Desulfovibrio* was dominant species, was found between PSEC and PSEM. The genus *Desulfovibrio* was also found in San Francisco Bay sediment, which can use acetate as an electron donor and carbon source for growth (Sun et al., 2000). *Desulfovibrio* is capable of oxidizing acetate, and its presence might be related to acetate oxidation in this work. A relative higher level of *Synergistaceae* (5.49%), *Dethiosulfovibrionaceae* (1.15%) and *Anaerolinaceae* (3.81%) were recovered in PSEC compared with PSEM. *Synergistaceae* and *Dethiosulfovibrionaceae* mainly consisted of the genera *Cloacibacillus* (99%) and *Aminobacterium* (99%), respectively. *Cloacibacillus* and *Aminobacterium* have also been

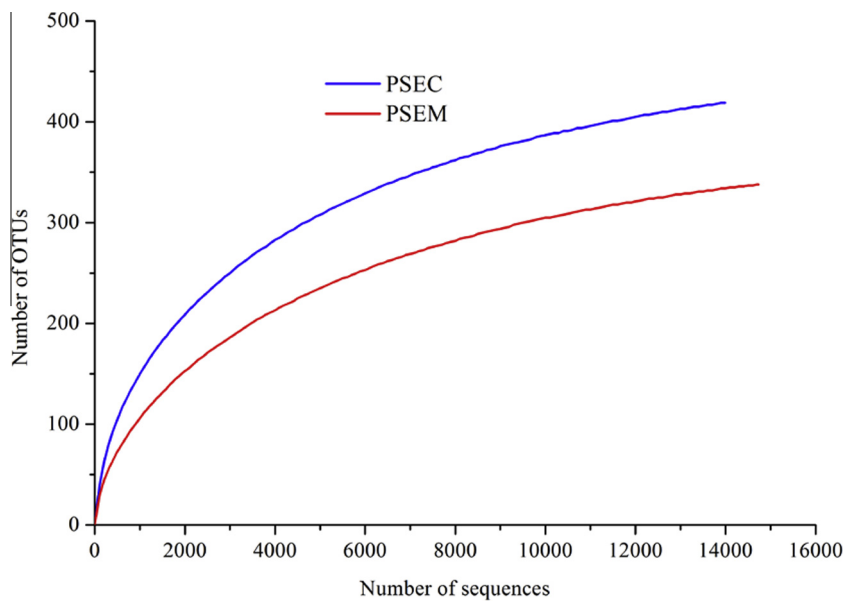


Fig. 3. Rarefaction curves for bacterial communities. The OTUs were defined by 0.03 distance irrespective of the non-specific amplification sequences.

Table 4

Comparison of the diversity of microbial community based on 0.03 distance irrespective of the non-specific amplification sequences.

	OTUs	Coverage (%)	CHA01 richness estimation	Shannon diversity
PSEC	419	97.1	471	3.59
PSEM	338	97.7	380	2.66

isolated from anaerobic reactors of a wastewater treatment plant, which were identified as amino-acid-degrading bacteria (Baena et al., 1998; Ganesan et al., 2008). *Anaerolinaceae* has also been detected in mesophilic anaerobic digester treating food waste, which can decompose carbohydrates in food waste via fermentation (Yi et al., 2014). Since no protein, amino acids and carbohydrate were added to the medium, *Cloacibacillus*, *Aminobacterium*

and *Anaerolinaceae* might be related to the degradation of carbohydrates or amino acids in the dead cells.

A relative higher abundance of *Acholeplasmataceae*, *Comamonadaceae* and *Pseudomonadaceae* in PSEM was observed when compared with PSEC. *Acholeplasmataceae* and *Comamonadaceae* were mainly consisted of the genera *Acholeplasma* and *Diaphorobacter*, respectively. *Acholeplasma* and *Diaphorobacter* were

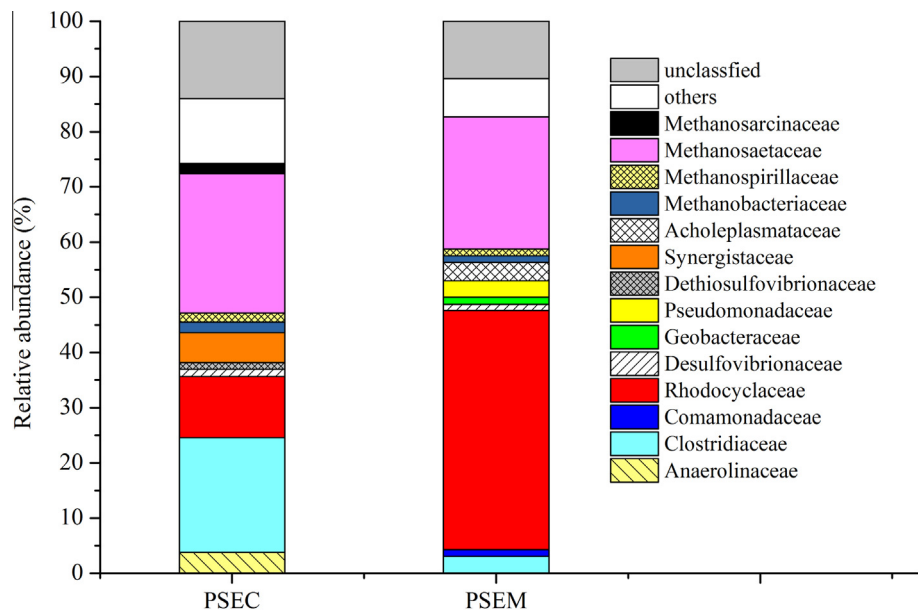


Fig. 4. Taxonomic level of microbial communities. Family accounting for less than 1% of total composition was represented as “others”.

also found in the methanogenesis from nonproductive coal and radionuclide-contaminated subsurface sediments, respectively (Jones et al., 2010; Akob et al., 2008). However, the role of these two species in conversion of acetate to methane was unknown. *Pseudomonadaceae* was largely composed of the genus *Pseudomonas* (99.2%). *Pseudomonas* has been shown to reduce Fe(III) with hydrogen as the substrate (Lovley, 2006), while its ability to metabolize acetate with Fe(III) as the electron acceptor was not reported.

A higher percentage of *Clostridiaceae* (20.77%) was observed in PSEC compared with PSEM (3.06%). *Clostridiaceae* largely consisted of the genus *Clostridium* (96%), which was also demonstrated to perform acetate oxidation in the presence of hydrogenotrophic methanogen (Hattori, 2008). The finding combined with the hydrogenotrophic *Methanobacteriaceae* identified in this work showed that the pathway of acetate oxidation to methane could occur in PSEC.

Recent studies showed that the addition of magnetite to rice paddy soil resulted in the accelerated methane production with specific enrichment of *Geobacter* and *Methanosarcina* (Kato et al., 2012; Zhou et al., 2014). Here, the addition of magnetite and acetate to paddy soil presented an apparent discrepancy with previous reports in microbial community structure. The dramatic enrichment of *Rhodocyclaceae* (66.77%) was observed in PSEM compared with PSEC (24.74%). The genera related to *Rhodocyclaceae* were mostly comprised of *Thauera* and *Dechloromonas* in this work. The sequences related to *Methanosaeta* (23.96%) were also recovered in PSEM. It is known that *Methanosaeta* can accept electrons from *Geobacter* via direct IET for the reduction of CO₂ to methane

(Rotaru et al., 2014). However, the results obtained in this work showed that only 1.28% of *Geobacter* was observed in PSEM. Thus, the finding demonstrated that direct IET in *Geobacter* might not be the predominant pathway for methanogenesis.

The dominant species, *Thauera* and *Dechloromonas*, have been reported to have capacity to reducing Fe(III) using acetate as electric donor under anaerobic conditions (Hori et al., 2009; Ma et al., 2014). These two species detected here indicated a strong possibility that they were associated with the Fe(III) reduction. However, it is unknown so far how the relationship occurred between *Rhodocyclaceae* and *Methanosaeta*. It is possible that *Thauera* and/or *Dechloromonas* can perform electric syntrophy with *Methanosaeta* facilitating methanogenesis via direct IET in a similar manner to *Geobacter* (Rotaru et al., 2014). However, this hypothesis could not be proved in this work. Further research is necessary to depict the IET mechanisms for methanogenesis using defined co-cultures or nucleic stable isotope probing.

3.3. Degradation of the effluents from the hydrogen-producing stage

The artificial medium and the effluents of hydrogen-producing stage were applied to evaluate the methanogenic performance of the paddy soil enrichments. PSEM improved methane production from the artificial medium in two cycles of incubation (Fig. 5). In the first incubation cycle, the amount of methane (29.8 mL) ultimately produced from the artificial medium by PSEM was higher than that by PSEC (11 mL). During the second incubation cycle, PSEM produced 32.7 mL of methane, while only 3.6 mL of methane

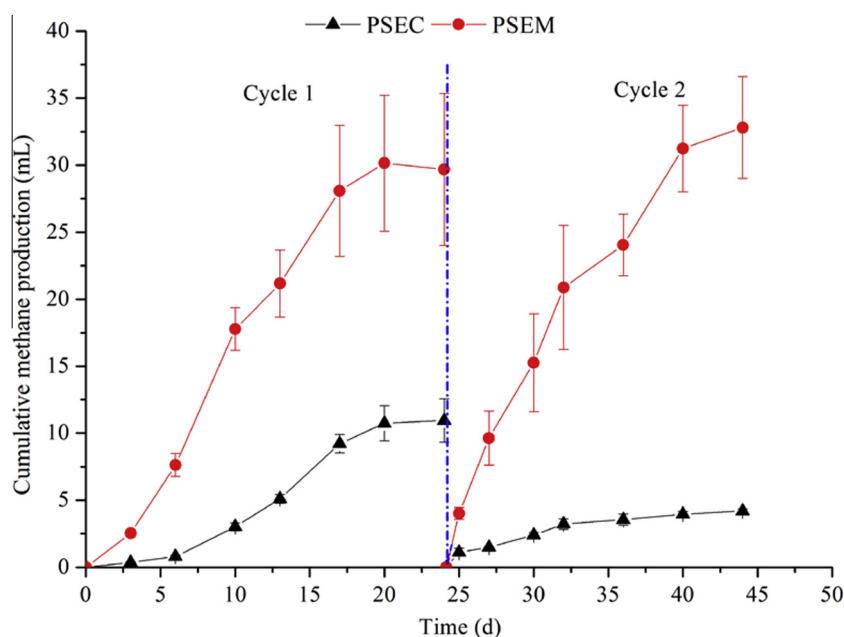


Fig. 5. Profiles of cumulative methane production from the artificial medium in the repeated batch cultivation.

Table 5

Comparison of methane production rate and artificial medium degradation during the repeated batch cultivation.

	Rm (mmol/d)	Ethanol (mM)	Acetate (mM)	Propionate (mM)	Butyrate (mM)	Caproate (mM)
<i>PSEC</i>						
Cycle 1	0.043	0	29.39 ± 0.49	10.42 ± 0.1	10.09 ± 0.09	1.47 ± 0.09
Cycle 2	0.017	14.33 ± 1.95	47.44 ± 0.73	16.77 ± 0.10	17.09 ± 0.18	1.21 ± 0.09
<i>PSEM</i>						
Cycle 1	0.106	0	7.44 ± 5.37	11.77 ± 0.83	12.91 ± 1.82	4.40 ± 1.64
Cycle 2	0.111	10.20 ± 7.81	20.49 ± 10.37	18.44 ± 0.73	21.09 ± 1.45	3.62 ± 1.72

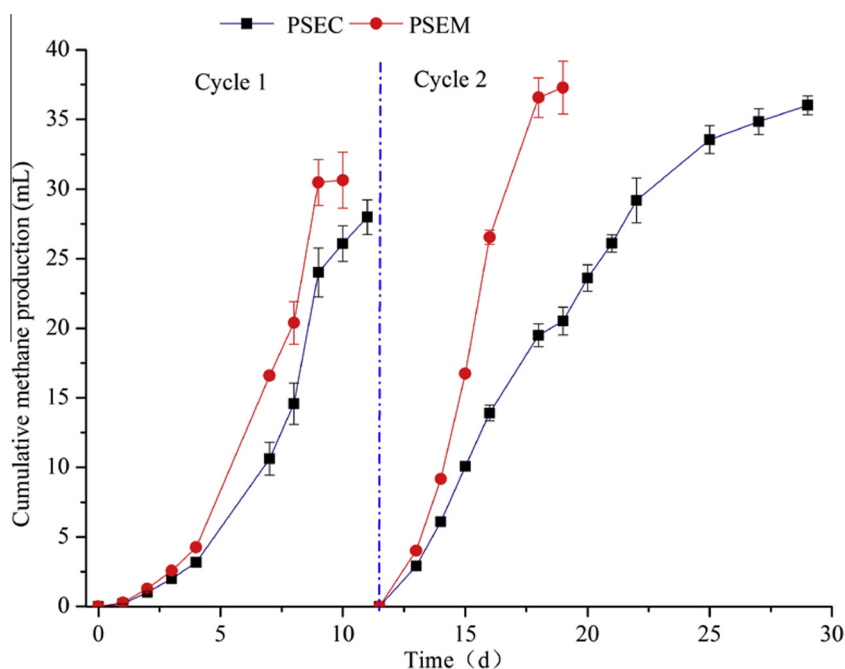


Fig. 6. Profiles of cumulative methane production from the effluents of hydrogen-producing stage in the repeated batch cultivation.

was produced by PSEC at the end of incubation. The maximum methane production rate in PSEM was also significantly higher (1.5 times higher in the first incubation cycle and 5.5 times higher in the second incubation cycle) than in the corresponding PSEC (Table 5).

As for the experiments feeding with the effluents, PSEM reduced the time course of methane production in two cycles of incubation. As shown in Fig. 6, during the first cycle of incubation, PSEM took 10 d to produce 31 mL of methane. In the second cycle, methane production stabilized after 8 d, and 37 mL of methane was produced. However, the ultimate amount of methane (28 mL) formed by PSEC was produced after 11 days in the first cycle. After 18 days, methane production achieved the maximum, which was 36 mL in the second cycle. Additionally, Table 6 shows that PSEM accelerated methane production in terms of the production rate. The maximum methane production rate in PSEM was higher (0.2 times higher in the first cycle and 1.7 times higher in the second cycle) than that in the corresponding PSEC. These results demonstrated the application potential of PSEM for conversion of the effluents from hydrogen-producing stage to methane. Baek et al. (2014) showed the enhanced methanogenic rate of activate sludge by adding the enriched iron-reducing bacteria consortium with ferric citrate. The findings obtained in this work also indicated other potential of PSEM for bioaugmentation treatment to improve the methanogenic performance of AD.

To analyze why methane production profiles from the artificial medium were significantly different from those from the effluents, the degradation of ethanol and VFAs in both the artificial medium and the effluents was further determined. Table 5 shows that propionate and butyrate were not efficiently removed in both groups supplemented with the artificial medium at each cycle. Considerable amounts of acetate were accumulated at each incubation cycle fed with the artificial medium. It has been reported that the accumulated acetate inhibited not only degradation of propionate and butyrate but also acetate itself degradation (Fukuzaki et al., 1990a, 1990b; Wang et al., 1999). Thus, the methanogenic inhibition might attribute to the accumulated acetate in this work. The relative higher methane yield in PSEM indicated that the threshold concentration of acetate inhibition may be higher than that of PSEC.

It should note that both ethanol and valerate were completely degraded in two groups supplemented with the effluents at each incubation cycle (Table 6). A relative higher removal of acetate, propionate and butyrate were also observed in both groups fed with the effluents compared with those fed with the artificial medium. This provided additional evidence that the degradation of acetate could alleviate the inhibition on the degradation of both butyrate and propionate. Previous reports also showed that the addition of iron oxide accelerated the methanogenesis from activated sludge with specific enrichment of iron-reducing bacteria (Baek et al., 2014). In this work, the effluents from the hydrogen-producing

Table 6
Comparison of methane production rate and effluent degradation during the repeated batch cultivation.

	Rm (mmol/d)	Acetate (mM)	Propionate (mM)	Butyrate (mM)	Caproate (mM)
<i>PSEC</i>					
Cycle 1	0.200	9.02 ± 1.22	2.71 ± 0.21	2.36 ± 0.09	2.41 ± 0.34
Cycle 2	0.145	0.49 ± 0.12	5.00 ± 0.31	0.36 ± 0.09	0.95 ± 0.52
<i>PSEM</i>					
Cycle 1	0.234	0.24 ± 0.12	3.85 ± 0.10	0.55 ± 0.09	0.21 ± 0.07
Cycle 2	0.387	0.24 ± 0.12	1.67 ± 0.42	0.64 ± 0.09	0.52 ± 0.17

stage consisted of large diversity of bacteria. Some iron-reducing bacteria from the effluents might be enriched due to the addition of magnetite, thus contributing to the accelerated removal of VFAs and rapid methanogenesis. Further experiments will be conducted to prove this case.

Interestingly, minor amounts of caproate were produced at each incubation cycle fed with the artificial medium and the effluents, indicating that there was a caproate-producing pathway occurred during the incubation. It is known that *Clostridium kluyveri* has been described as their ability to elongation ethanol and acetate to caproate (Seedorf et al., 2008). It is possible that some member of *Clostridium* identified in enrichment cultures (Fig. 4) might also produce caproate in the similar manner as *Clostridium kluyveri*.

The findings presented here showed that PSEM has practical application potential in enhancing methanogenesis. The findings will also be beneficial for engineering processes of biogas digester to accelerate the removal of waste biomass.

4. Conclusions

Nanoscale magnetite particles can facilitate methane production from acetate in a dose-independent manner, concomitant with specific enrichment of an unusual microbial consortia from the paddy soil. The dominant *Rhodocyclaceae*-related populations might be responsible for acetate degradation in the similar manner as *Geobacter*. High concentrations of acetate inhibited methane production not only from acetate itself but also from propionate and butyrate in the artificial medium. However, a significant increase in the maximum methane production rate from the effluents of hydrogen-producing stage in the two-stage AD showed that PSEM had remarkable application prospects in enhancing methanogenic performance of AD.

Acknowledgements

The authors appreciate Associated Prof. Li Zhuang (Guangdong Institute of Eco-Environmental and Soil Sciences) for providing paddy soil. This work was funded by the National Natural Science Foundation of China (No. 21307143, No. 41276143), 863 Project (No. 2011AA060905), Key Deployment Project of the Chinese Academy of Sciences (No. KGXC2-EW-317), Key Research Program of the Chinese Academy of Sciences (No. KGZD-EW-304).

References

- Akob, D.M., Mills, H.J., Gihring, T.M., Kerkhof, L., Stucki, J.W., Anastácio, A.S., Chin, K.-J., Küsel, K., Palumbo, A.V., Watson, D.B., Kostka, J.E., 2008. Functional diversity and electron donor dependence of microbial populations capable of U(VI) reduction in radionuclide-contaminated subsurface sediments. *Appl. Environ. Microbiol.* 74 (10), 3159–3170.
- APHA, 1998. Standard Methods for the Examination of Waste and Wastewater, 20th ed. American Public Health Association, Washington (DC, USA).
- Baek, G., Kim, J., Lee, C., 2014. Influence of ferric oxyhydroxide addition on biometanation of waste activated sludge in a continuous reactor. *Bioresour. Technol.* 166, 596–601.
- Baena, S., Fardeau, M.L., Labat, M., Ollivier, B., Thomas, P., Garcia, J.L., Patel, B.K.C., 1998. Aminobacterium colombiense gen. nov. sp. nov., an amino acid-degrading anaerobe isolated from anaerobic sludge. *Anaerobe* 4 (5), 241–250.
- Caporaso, J.G., Kuczynski, J., Stombaugh, J., Bittinger, K., Bushman, F.D., Costello, E.K., Fierer, N., Pena, A.G., Goodrich, J.K., Gordon, J.I., Huttley, G.A., Kelley, S.T., Knights, D., Koenig, J.E., Ley, R.E., Lozupone, C.A., McDonald, D., Muegge, B.D., Pirrung, M., Reeder, J., Sevinsky, J.R., Turnbaugh, P.J., Walters, W.A., Widmann, J., Yatsunenko, T., Zaneveld, J., Knight, R., 2010. QIIME allows analysis of high-throughput community sequencing data. *Nat. Methods* 7 (5), 335–336.
- Dareioti, M.A., Kornaros, M., 2014. Effect of hydraulic retention time (HRT) on the anaerobic co-digestion of agro-industrial wastes in a two-stage CSTR system. *Bioresour. Technol.* 167, 407–415.
- DeSantis, T.Z., Hugenholtz, P., Larsen, N., Rojas, M., Brodie, E.L., Keller, K., Huber, T., Dalevi, D., Hu, P., Andersen, G.L., 2006. Greengenes, a chimera-checked 16S rRNA gene database and workbench compatible with ARB. *Appl. Environ. Microbiol.* 72 (7), 5069–5072.
- Edgar, R.C., 2013. UPARSE: highly accurate OTU sequences from microbial amplicon reads. *Nat. Methods* 10 (10), 996–998.
- Edgar, R.C., Haas, B.J., Clemente, J.C., Quince, C., Knight, R., 2011. UCHIME improves sensitivity and speed of chimera detection. *Bioinformatics* 27, 2194–2200.
- Fukuzaki, S., Nishio, N., Nagai, S., 1990a. Kinetics of the methanogenic fermentation of acetate. *Appl. Environ. Microbiol.* 56 (16), 3158–3163.
- Fukuzaki, S., Nishio, N., Shobayashi, M., Nagai, S., 1990b. Inhibition of the fermentation of propionate to methane by hydrogen, acetate, and propionate. *Appl. Environ. Microbiol.* 56 (3), 719–723.
- Ganesan, A., Chaussonnerie, S., Tarrade, A., Dauga, C., Bouchez, T., Pelletier, E., Le Paslier, D., Sghir, A., 2008. *Cloacibacillus evryensis* gen. nov., sp. nov., a novel asaccharolytic, mesophilic, amino-acid-degrading bacterium within the phylum 'Synergistetes', isolated from an anaerobic sludge digester. *Int. J. Syst. Evol. Microbiol.* 58 (9), 2003–2012.
- Hattori, S., 2008. Syntrophic acetate-oxidizing microbes in methanogenic environments. *Microbes Environ.* 23 (2), 118–127.
- Hori, T., Muller, A., Igarashi, Y., Conrad, R., Friedrich, M.W., 2009. Identification of iron-reducing microorganisms in anoxic rice paddy soil by ^{13}C -acetate probing. *ISME J.* 4 (2), 267–278.
- Jones, E.J.P., Voytek, M.A., Corum, M.D., Orem, W.H., 2010. Stimulation of methane generation from nonproductive coal by addition of nutrients or a microbial consortium. *Appl. Environ. Microbiol.* 76 (21), 7013–7022.
- Kang, Y.S., Risbud, S., Rabolt, J.F., Stroeve, P., 1996. Synthesis and characterization of nanometer-size Fe_3O_4 and $\gamma\text{-Fe}_2\text{O}_3$ particles. *Chem. Mater.* 8 (9), 2209–2211.
- Kato, S., Hashimoto, K., Watanabe, K., 2012. Methanogenesis facilitated by electric syntrophy via (semi)conductive iron-oxide minerals. *Environ. Microbiol.* 14 (7), 1646–1654.
- Kwietniewska, E., Tys, J., 2014. Process characteristics, inhibition factors and methane yields of anaerobic digestion process, with particular focus on microalgal biomass fermentation. *Renew. Sustain. Energy Rev.* 34, 491–500.
- Lovley, D., 2006. Dissimilatory Fe(III) - and Mn(IV) -Reducing Prokaryotes. In: Dworkin, M., Falkow, S., Rosenberg, E., Schleifer, K.-H., Stackebrandt, E. (Eds.), *The Prokaryotes*. Springer, New York, pp. 635–658.
- Ma, C., Yu, Z., Lu, Q., Zhuang, L., Zhou, S.-G., 2014. Anaerobic humus and Fe(III) reduction and electron transport pathway by a novel humus-reducing bacterium, *Thauera humireducens* SgZ-1. *Appl. Microbiol. Biotechnol.*, 1–10.
- Magoč, T., Salzberg, S.L., 2011. FLASH: fast length adjustment of short reads to improve genome assemblies. *Bioinformatics* 27 (21), 2957–2963.
- Massanet-Nicolau, J., Dinsdale, R., Guwy, A., Shipley, G., 2013. Use of real time gas production data for more accurate comparison of continuous single-stage and two-stage fermentation. *Bioresour. Technol.* 129, 561–567.
- Merlino, G., Rizzi, A., Schievano, A., Tenca, A., Scaglia, B., Oberti, R., Adani, F., Daffonchio, D., 2013. Microbial community structure and dynamics in two-stage vs single-stage thermophilic anaerobic digestion of mixed swine slurry and market bio-waste. *Water Res.* 47 (6), 1983–1995.
- Peiffer, Jason A., Sporb, Aymé, Korenb, Omry, Jin, Zhao., Tringed, Susannah Green., Dangle, Jeffery L., Buckler, Edward S., Ley, R.E., 2013. Diversity and heritability of the maize rhizosphere microbiome under field conditions. *Proc. Natl. Acad. Sci. U.S.A.* 110, 6548–6553.
- Rotaru, A.-E., Shrestha, P.M., Liu, F., Shrestha, M., Shrestha, D., Embree, M., Zengler, K., Wardman, C., Nevin, K.P., Lovley, D.R., 2014. A new model for electron flow during anaerobic digestion: direct interspecies electron transfer to *Methanosaeta* for the reduction of carbon dioxide to methane. *Energy Environ. Sci.* 7 (1), 408–415.
- Ruile, S., Schmitz, S., Mönch-Tegeder, M., Oechsner, H., 2015. Degradation efficiency of agricultural biogas plants – a full-scale study. *Bioresour. Technol.* 178, 341–349.
- Seedorf, H., Fricke, W.F., Veith, B., Bruggemann, H., Liesegang, H., Strittmatter, A., Miethke, M., Buckel, W., Hinderberger, J., Li, F., Hagemeyer, C., Thauer, R.K., Gottschalk, G., 2008. The genome of *Clostridium kluyveri*, a strict anaerobe with unique metabolic features. *Proc. Natl. Acad. Sci. U.S.A.* 105 (6), 2128–2133.
- Sieber, J.R., McInerney, M.J., Gunsalus, R.P., 2012. Genomic insights into syntrophy: the paradigm for anaerobic metabolic cooperation. *Annu. Rev. Microbiol.* 66 (1), 429–452.
- Sun, B., Cole, J.R., Sanford, R.A., Tiedje, J.M., 2000. Isolation and characterization of desulfovibrio dechloracetivorans sp. nov., a marine dechlorinating bacterium growing by coupling the oxidation of acetate to the reductive dechlorination of 2-chlorophenol. *Appl. Environ. Microbiol.* 66 (6), 2408–2413.
- Wang, Q., Kuninobu, M., Ogawa, H.I., Kato, Y., 1999. Degradation of volatile fatty acids in highly efficient anaerobic digestion. *Biomass Bioenergy* 16 (6), 407–416.
- Wang, Q., Garrity, G.M., Tiedje, J.M., Cole, J.R., 2007. Naive Bayesian classifier for rapid assignment of rRNA sequences into the new bacterial taxonomy. *Appl. Environ. Microbiol.* 73 (16), 5261–5267.
- Wang, Y., Zhang, Y., Meng, L., Wang, J., Zhang, W., 2009. Hydrogen-methane production from swine manure: effect of pretreatment and VFAs accumulation on gas yield. *Biomass Bioenergy* 33 (9), 1131–1138.
- Yang, Z., Guo, R., Xu, X., Fan, X., Luo, S., 2011. Hydrogen and methane production from lipid-extracted microalgal biomass residues. *Int. J. Hydrogen Energy* 36 (5), 3465–3470.
- Yi, J., Dong, B., Jin, J., Dai, X., 2014. Effect of increasing total solids contents on anaerobic digestion of food waste under mesophilic conditions: performance and microbial characteristics analysis. *PLoS ONE* 9 (7), e102548.
- Zhou, S., Xu, J., Yang, G., Zhuang, L., 2014. Methanogenesis affected by the co-occurrence of iron(III) oxides and humic substances. *FEMS Microbiol. Ecol.* 88 (1), 107–120.